

Optimization of the active region of interband cascade lasers emitting in the MIR

Krzysztof Ryczko and Grzegorz Sęk*

OSN Lab, Department of Experimental Physics, Faculty of Fundamental Problems of Technology,
Wrocław University of Science and Technology,
Wybrzeże Wyspiańskiego 27, 50-370 Wrocław, Poland

ABSTRACT

Interband cascade lasers (ICLs) are efficient mid-infrared (MIR) semiconductor light sources based typically on InAs and GaInSb materials forming a broken gap system and hence type II quantum wells (QWs) being the active part in this kind of emitters. There has already been achieved a significant progress in the performance of ICLs, driven mainly by the gas sensing applications and originating from their unique operational characteristics when especially compared to quantum cascade lasers. However, there are still growing demands with respect to laser sources in the MIR and new areas of applications evolve, all of which stimulate the efforts to improve the performance of such devices and to search for completely new solutions which could offer properties hardly reachable with existing structures. Here, by using *k*-*p* theory employing strain and band structure engineering of various In(As,Sb) and (Ga,In)(As,Sb) type II materials' combinations there will be considered several novel designs of the active region of ICLs. These calculations show that such new features can be obtained as fully strain-free ICL devices, significant extension of the emission spectral range, polarization independent gain in the MIR or enhanced sensitivity of radiative processes rates to external electric field to be exploited in bias-controlled mode-locked ICLs. The respective type II QW designs are proposed and discussed.

Keywords: gas sensing, interband cascade laser, active region, type II quantum well, band structure, mode-locking.

1. INTRODUCTION

Currently, there exist a rapidly-growing demand for efficient semiconductor lasers emitting in the mid-infrared (MIR) wavelength range, especially between 3 and 6 μm . One of already established sources in this region are interband cascade lasers (ICLs).^{1,2} They combine a long upper-level recombination lifetime of a conventional diode laser with a voltage-efficient cascading scheme, borrowed from a quantum cascade laser, which however, in contrast to the latter produces coherent light via intersubband transitions. Over the past couple of years, there has been achieved significant progress in the performance of MIR lasers leading to, for example: (i) low electric power consumption,³ (ii) record low threshold current densities,¹ (iii) single mode, continuous wave (cw) and high power operation at room or even elevated temperatures,^{4,6} (iv) CW operation at room temperature and above, for wavelengths up to at least 5.6 μm ;⁷ (v) broad spectral tunability;⁸ (vi) pulsed room temperature laser operation with ultralow threshold currents in the range from 2.8 to 7 μm .^{1,6,9} Recently, there have also been discussed several modified structures of ICL's active region aiming at further improvements in characteristics and extension of the application fields, as for instance designs allowing for strain control or fully unstrained devices.^{10,11}

Efficient MIR semiconductor lasers as the ICLs have considerable advantages in terms of volume, weight, simplicity of design, reliability, and cost. Commercial markets for such devices include environmental monitoring,¹² industrial process control,¹³ exhaled breath analysis for medical diagnostics,¹⁴ or trace gas detection.^{15,16} Also, an increasingly important optical sensing method utilizing ICLs is tunable diode laser absorption spectroscopy, which allows for selective gas species detection in real time, with sensitivities up to particle per trillion, using single mode semiconductor lasers, which can be tuned rapidly by varying the drive current.¹⁷

*grzegorz.sek@pwr.edu.pl; phone +48 71 320 45 73; fax 48 71 328 36 96; <http://osn.pwr.edu.pl/>

Nowadays, strong interest is especially directed towards mid-infrared dual-comb spectroscopy, which could revolutionize chemical sensing as well as high resolution spectroscopy.^{18,19} To obtain mid-infrared frequency combs different approaches are used.^{20,21} One of the possible solutions is the use of mode-locked lasers due to their ability to generate ultra-short light pulses at high repetition rates. Passive mode locking is commonly obtained by combining two elements, a laser amplifier which provides gain, and a saturable absorber forcing a pulsed emission. In that context, remarkable progress has been achieved within the last few years and various ideas towards realization of mode-locked ICL's appeared,²² and just recently there have been demonstrated the first mode-locked-ICL-based optical frequency combs operating in the 3–4 μm wavelength range.²³

However, the still increasing demands of the gas sensing applications or appearance of new application areas expecting new functionalities and better device and sensing system performance drive further developments of the lasers sources. In case of ICLs, some of these steps forward can be obtained by optimizing their active region, which in commonly exploited devices is composed of a cascade of type II quantum wells (QWs) made of broken gap materials, InAs and GaInSb, forming the so called “W-like” quantum well due to the shape band edge profile of InAs/GaInSb/InAs layers, with usually AlSb barriers. These, seem to reach their natural limits, therefore, paving the way towards a new calls of MIR lasers based on the ICL scheme requires new type II material solutions, which could offer properties hardly reachable by the state-of-the-art devices. In this paper, we make a short overview of such modifications in the active region o ICLs based on theoretical modeling of their electronic structure and fundamental optical properties, as well as predictions on expected improvements in the performance of the laser sources.

2. METHODOLOGY

All the considerations in this paper are based on eight-band $k \cdot p$ theory including strain. As such structures are typically grown along [001] direction this is regarded as the z-axis. In heterostructures such as InAs/GaSb-based quantum wells, the dispersion relations for electron and hole subbands along the directions in the plane are hybridized and mixed due to the coupling of the conduction and valence band states in different material layers. Therefore, our approach includes the multiband coupling and the respective states mixing. We quantize the Hamiltonian along the growth direction and use the three-point finite difference method with uniform meshes to solve the Schrödinger equation numerically. The materials' parameters are taken after Ref. 24. To investigate the optical transitions, we mainly examine the matrix elements of the envelope functions, which are primarily determined by the spatial overlap integral of the the electron and hole wave functions ($|\langle \Psi_e | \Psi_h \rangle|^2$). Further details on the calculation methodology can be found in Ref. 25.

3. RESULTS AND DISCUSSION

3.1 Exploiting new materials and strain engineering

Typical type II quantum well of the active region in an ICL is composed of two InAs layers to confine electrons and one GaInSb layer for confinement of holes, all usually surrounded by AlSb barrier. Such structures are called “W-shaped” as the potential profile resembles the “W” letter. The use of a double InAs layer for confinement of electrons increases the oscillator strength of the optical transitions, when compared to a single sequence of just InAs and GaInSb . The respective band diagrams of an exemplary structure and its fundamental confined states are shown in Fig. 1 compared to a type II structure with a single InAs layer to visualize the wave functions' overlap enhancement.

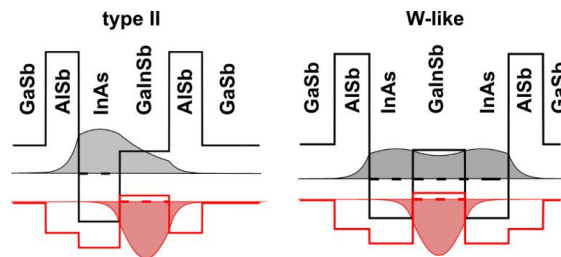


Figure 1. Band diagrams and the fundamental states wave functions in typical InAs/GaInSb QWs of type II (left) and W-shaped (right) designs.

As the entire system is nominally strained (independently of the used substrate, which is GaSb or InAs) on one hand, and on the other to obtain enough gain for lasing relatively large transition intensity (absorption) is needed, the layer thicknesses are usually very thin (in the range of 1-4 nm) and the In content in the GaInSb layer is kept below 40% (to do not exceed about 2% of the compressive strain). Figure 2 shows the dependence of the fundamental type II transition energy and the related squared overlap integral of the electron and hole wave functions versus the thickness of the InAs layer of a “W” quantum well (as this is the most efficient tuning parameter).

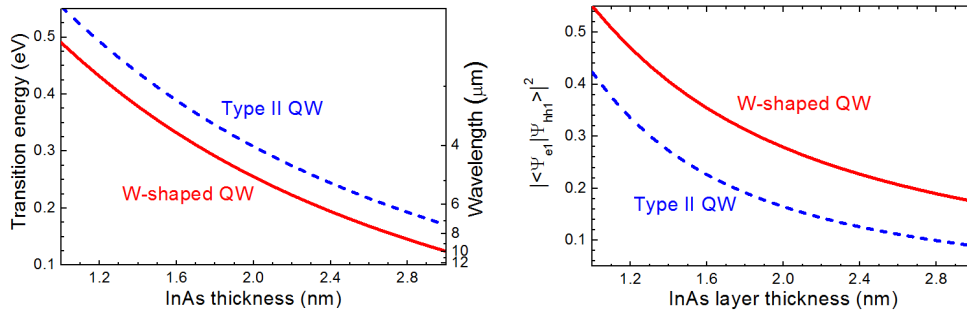


Figure 2. InAs layers’ thickness dependence of the transition energy (wavelength) – left, and squared wave functions’ overlap – right.

It can be seen, that nominally these type II structure can cover the spectral range of emission from below 2.5 to about 10 μm at least, and that using W-design allows pushing the active transition further to the infrared while increasing the transition oscillator strength significantly. However, when going beyond 6 μm the squared overlap gets below 0.2, which is already very low with respect to build enough gain and reach the lasing thresholds. Therefore, this is one of the main active region parameters requiring improvements.

In spite of the abovementioned successful development of ICLs utilizing such QWs, their apparently reached limitations, and hence, one of the routes to further exploit this kind of interband cascaded scheme is to modify the active material and use the strain engineering as an additional tool. We have proposed¹⁰ to use GaAsSb material for confinement of holes, which makes the QW layer tensely-strained, in contrast to GaInSb, where the amount of strain can be regulated by the composition. The tensile strain causes a reversed order of the valence band edges (the light band edge at $k = 0$ goes above the one for heavy holes), which in the quantum well where different effective masses are involved yet plus the states intermixing that the character of the QW ground state for holes can be continuously tuned from fully heavy hole (HH) to fully light hole (LH) character. Figure 3 shows schematically how the confinement potential changes in function of the arsenic content in the GaAsSb layers.

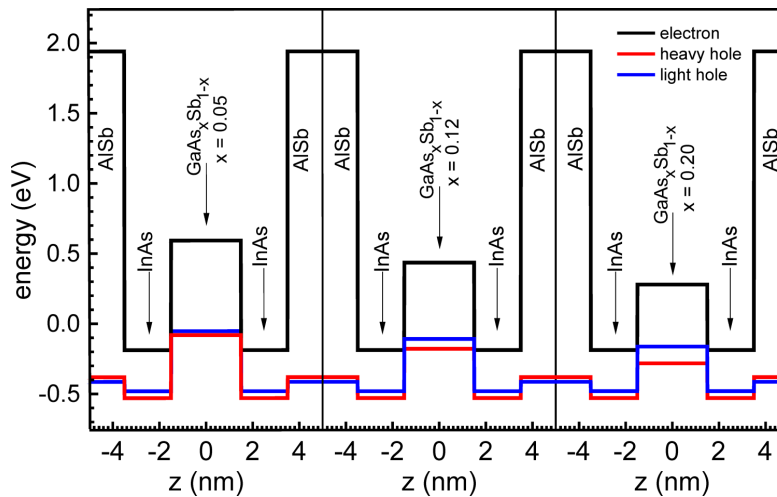


Figure 3. Band edge diagrams for three As contents in W-design InAs/GaAsSb/InAs QWs.

This has important consequences to all the optical properties, including also the wavelength tunability as well as the wave functions' overlaps. The latter are, in general, increased due to mainly the contribution of the light hole states to the lowest valence band confined state, i.e. a decreased effective mass translating into broader wave function extension and hence better overlap with the electron wave function. Figure 4 shows examples of the squared wave functions moduli for InAs/GaAsSb/InAs of two different compositions.

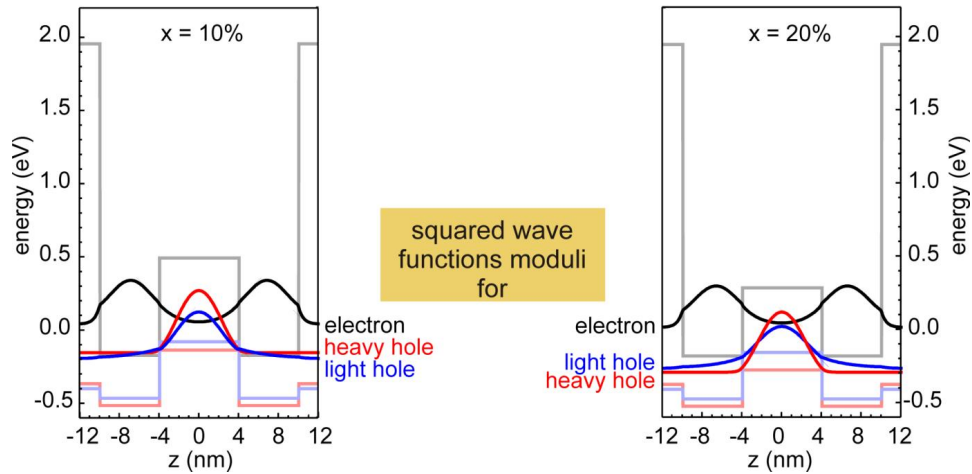


Figure 4. Squared moduli of the wave functions for InAs/GaAsSb/InAs QWs of two different compositions.

Figure 5 shows the spectral tunability of the optical transitions for the two lowest valence band states, which is at least as good as for GaInSb-containing QWs but with significantly larger oscillator strengths - the squared overlap integrals can be larger from about 20% at shorter wavelengths to even a factor 3-5 at longer wavelengths of the MIR.¹⁰ It is seen in Fig. 5 that for the particular example the ground state character switches from heavy into light hole for about 16% of arsenic. The bottom part of the figure plots the value of the strain in the given range of As contents in order to show that up to about 20% of arsenic they are well below 2%, i.e. realizable from the practical, epitaxial growth point of view.

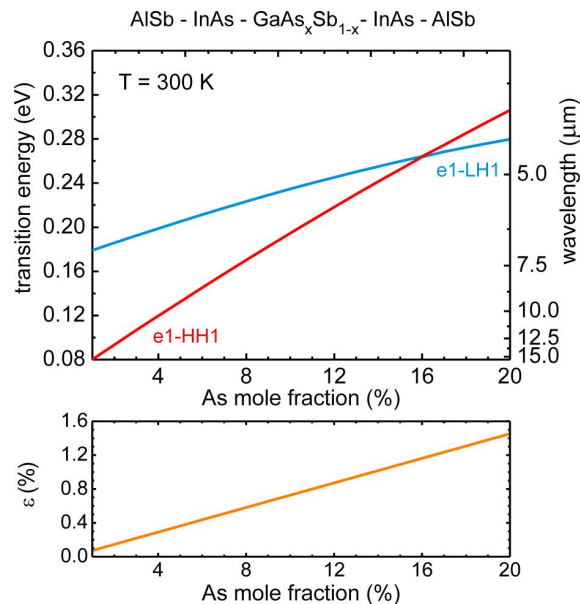


Figure 5. Transition energies (wavelengths) in function of the As content for InAs/GaAsSb/InAs QW; the amount of strain is shown at the bottom.

3.2 Tailoring the valence band mixing for polarization independence

The valence band states intermixing effects are even more important for the dispersion relations beyond $k = 0$, which contribute significantly to total absorption and hence the laser gain function in the conditions of high carrier concentrations as in operational devices. Therefore, in order to account for the mixing effects properly the respective contributions must be integrated over k . On the other hand, the optical transitions selection rules are polarization dependent and for the edge emitting devices the states mixing affects the ratio between the TE and TM linear polarizations – increasing the LH contribution makes the transition more TM polarized, which for typical compressive strain structures are dominated by heavy holes and hence the gain is also predominantly TE polarized. Using tensely-strained material of GaAsSb allows tailoring this dependence. To calculate the gain spectra the transitions rates are integrated k_{\parallel} for all the interband transitions, where the transitions rates are weighted by the corresponding population factor $[f_n^c(k_{\parallel}) - f_m^v(k_{\parallel})]$, where $f_n^c(k_{\parallel})$ and $f_m^v(k_{\parallel})$ are the Fermi distribution functions for electrons and holes, respectively, at given temperature. To include the spectral broadening in each transition caused by all sources of the electron scattering, we convolve the expression for the optical gain with Lorentzian line shape function over all the transition energies. Eventually, the optical gain is calculated for different carrier injection densities to simulate the experimental conditions. More details can be found in Ref. 26.

Tuning all the described parameters for the strain-controlled type II QW structures allows finding conditions where the TE and TM gain functions become equal, in some range of wavelengths at least. Figure 6 shows an example of the derived gain functions for W-design InAs(2.8 nm)/GaAs_{0.12}Sb_{0.88}(7 nm)/InAs(2.8 nm) QW. It is seen that gain in both polarizations is equal in the 3 μm range. This result paves the way towards polarization independent emitters or amplifiers in the MIR.

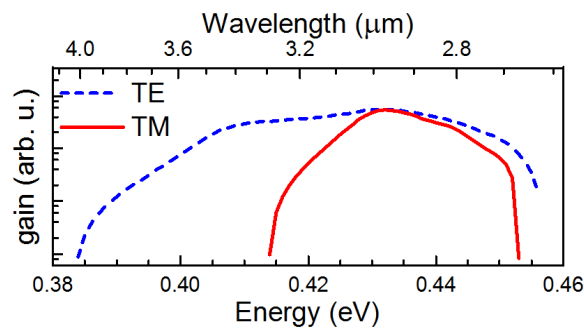


Figure 6. Transition energies (wavelengths) in function of the As content for InAs/GaAsSb/InAs QW; the amount of strain is shown at the bottom.²⁶

3.3 Enhanced electric field sensitivity for passive mode-locking

In order to realize a passively-mode locked device the absorbing medium dynamics should be much faster than the gain medium dynamics, i.e. $\tau_a \ll \tau_g$. One can consider using electric field as a tool to affect oscillator strength of the active optical transition, which is inversely proportional to its lifetime. However, to make such an approach efficient, high sensitivity of the tailored quantum structure to external bias is required. As the strain-engineered “W” structures involve more light-hole-like valence band states, their wave function is more extended in the real space in the z direction, and hence greater layers thicknesses can be taken into account. This then turns into higher sensitivity to external electric field. Figure 7 shows the calculated electric field dependence of the relative oscillator strength (with respect to case of zero electric field) and the related transition energy (emission wavelength) for W-design type II QW made of InAs(6 nm)/GaAs_{0.2}Sb_{0.8}(7nm)/InAs(3.6 nm). It is worth underlining, that the used QW layer thicknesses are indeed larger than those for InAs/GaInSb structures, and that the two InAs wells confining electrons are of different thicknesses. The latter is due to the electric field effect which in one of its directions makes this partly asymmetric system even more asymmetric (lower oscillator strength) and in the opposite symmetrize the structure and enhances the transitions oscillator strength (shorter lifetimes as required in the saturable absorber section). For the discussed case, a change of the oscillator strength by a factor of 5 could be obtained in the fields’ range of -100 to +100 kV/cm, which is promising from the point of view of the mode-locked operation. This is especially as it concerns the possible emission wavelengths of about 4 μm , i.e. in target range of many gas sensing applications. However, similar data can also be obtained in other ranges of MIR from about 2.5 to 6 μm at least.²⁷

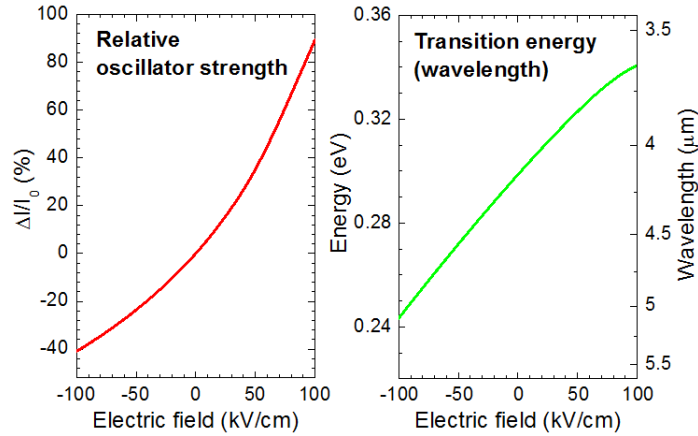


Figure 7. Electric field dependence of the fundamental transition oscillator strength (calculated with respect to the case without electric field) and transition energy (emission wavelength) for W-design InAs(6 nm)/GaAs_{0.2}Sb_{0.8}(7nm)/InAs(3.6 nm) QW.²⁷

3.4 Strain-free active region

As the involvement of compressively and tensely strained materials is possible in these MIR emitting type II structures, one can combine both into one system and aim at a fully strain-free system. This would be crucial for growth technology and easier multilayer device fabrication, but it also opens up new possibilities of the band structure and optical properties engineering, as the layers' critical thickness is not a limiting factor anymore.

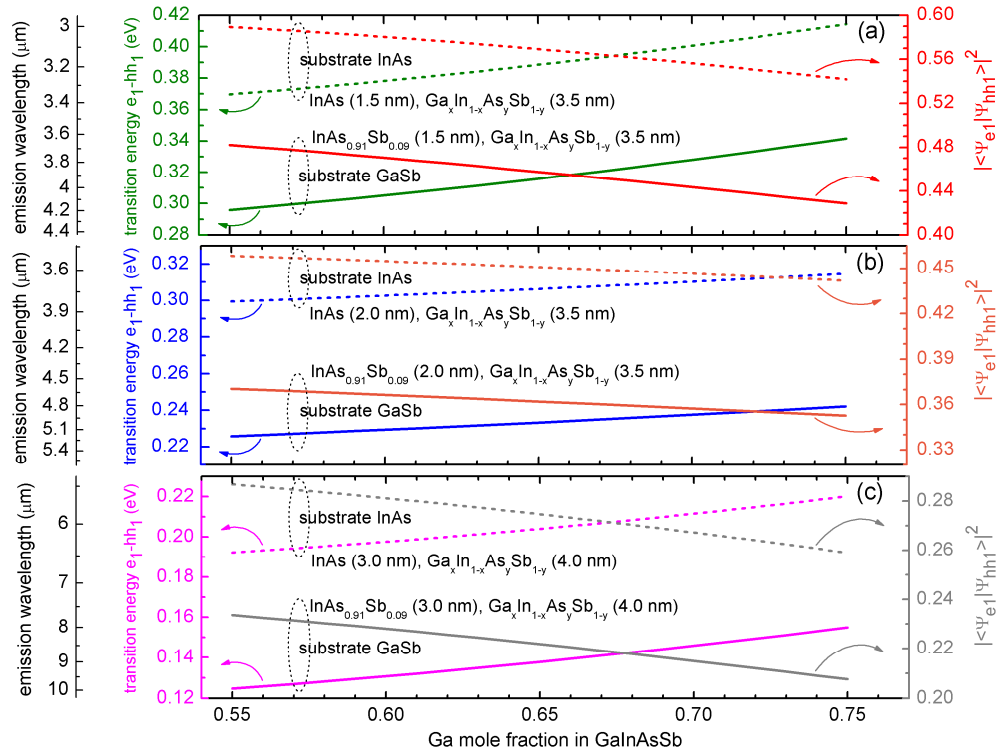


Figure 8. Optical transition energy (and the related emission wavelength) as well as the squared overlap integrals for various In(As,Sb)/(Ga,In)(As,Sb)/In(As,Sb) with different layers' thicknesses and compositions assuring the lattice matching to an InAs or GaSb substrate.

In addition, when quaternary materials are included, the energy gaps can be tuned independently, which connected with varying the layers' thicknesses give basically a full freedom in the emission wavelength coverage for such QWs. As the two kinds of substrates used, InAs and GaSb, differ slightly in their lattice constants, the unstrained system must be different in both cases. For holes' confinement material it means a different composition of GaInAsSb layer, whereas for electrons' QW it can be or pure InAs (for the InAs substrate) or InAs_{0.91}Sb_{0.09} (lattice-matched to GaSb).

Figure 8 shows the results of calculations for numerous type II quantum wells and their various parameters, however all for compositions lattice-matched to InAs or GaSb. It proves, on one hand, that indeed the unstrained QWs can be designed for any wavelength of the 3-10 μm range, and beyond, but on the other hand, that the transitions oscillator strength (expressed via the squared wave functions' overlap integrals) are significant in all cases, i.e. suitable for the use in the active region of ICLs.

4. SUMMARY

We have overviewed a couple of examples of the band structure and strain modifications via introducing new materials into the active part of interband cascade lasers emitting in the MIR. Such an extension gives knobs to tune various optical properties, which can bring the ICLs into currently unavailable performance characteristics, and which then turn into new functionalities and hence possible new applications in the laser-based optical spectroscopy and sensing. For instance, we have shown that by using tensely-strained GaAsSb material for the confinement of holes the polarization selection rules can be tailored and as a consequence also the TE and TM gains of the edge emitting devices. This kind of type II QWs appeared also suitable for bias controlled architecture of a mode-locked ICL which can become a breakthrough tool in the dual comb spectroscopy methods. Eventually, pushing the material engineering even further and involving quaternary GaInAsSb allows obtaining unstrained active regions, a step towards fully strain-free ICLs, which can be a milestone in both the fabrication technology but also the system parameters tunability, which could not be reached in the normally strained structures.

ACKNOWLEDGEMENTS

This work has been supported by iCspec project which had received funding from the European Union's Horizon 2020 Research and Innovation Program under grant agreement No 636930, and by the National Science Centre of Poland within Grant No. 2014/15/B/ST7/04663.

REFERENCES

- [1] Vurgaftman, I., Weih, R., Kamp, M., Meyer, J. R., Canedy, C. L., Kim, C. S., Kim, M., Bewley, W. W., Merritt, C. D., Abell, J., Höfling, S., "Interband cascade lasers", *J. Phys. D: Appl. Phys.* 48(12), 123001 (2015).
- [2] Bauer, A., Rößner, K., Lehnhardt, T., Kamp, M., Höfling, S., Worschech, L., Forchel, A., "Mid-infrared semiconductor heterostructure lasers for gas sensing applications", *Semicond. Sci. Technol.* 26, 014032 (2011).
- [3] Vurgaftman, I., Bewley, W. W., Canedy, C. L., Kim, C. S., Kim, M., Merritt, C. D., Abell, J., Lindle, J. R., Meyer, J. R., "Rebalancing of internally generated carriers for mid-infrared interband cascade lasers with very low power consumption", *Nature Commun.* 2, 585 (2011).
- [4] Bewley, W. W., Kim, C. S., Canedy, C. L., Merritt, C. D., Vurgaftman, I., Abell, J., Meyer, J. R., Kim, M., "High-power, high-brightness continuous-wave interband cascade lasers with tapered ridges", *Appl. Phys. Lett.* 103, 111111 (2013).
- [5] Weih, R., Kamp, M., Höfling, S., "Interband cascade lasers with room temperature threshold current densities below 100 A/cm²", *Appl. Phys. Lett.* 102, 231123 (2013).
- [6] Kim, C. S., Bewley, W. W., Merritt, C. D., Canedy, C. L., Warren, M., Vurgaftman, I., Meyer, J. R., Kim, M., "Improved mid-infrared interband cascade light-emitting devices", *Optical Engineering* 57(1), 011002 (2017).
- [7] Bewley, W. W., Canedy, C. L., Kim, C. S., Kim, M., Merritt, C. D., Abell, J., Vurgaftman, I., Meyer, J. R., "Continuous-wave interband cascade lasers operating above room temperature at $\lambda = 4.7\text{-}5.6 \mu\text{m}$ ", *Opt. Express* 20(3), 3235-3240 (2012).

- [8] Jiang, Y., Li, L., Tian, Z., Ye, H., Zhao, L., Yang, R. Q., Mishima, T. D., Santos, M. B., Johnson, M. B., Mansour, K., "Influence of carrier concentration on properties of InAs waveguide layers in interband cascade laser structures", *J. Appl. Phys.* 115, 113101 (2014).
- [9] Dallner, M., Hau, F., Höfling, S., Kamp, M., "InAs-based interband-cascade-lasers emitting around 7 μm with threshold current densities below 1 kA/cm^2 at room temperature", *Appl. Phys. Lett.* 106, 041108 (2015).
- [10] Ryczko, K., Sęk, G., Misiewicz, J., "Novel design of type-II quantum wells for mid-infrared emission with tensile-strained GaAsSb layer for confinement of holes", *Appl. Phys. Express* 8, 121201 (2015).
- [11] Ryczko, K., Sęk, G., "Towards unstrained interband cascade lasers", *Appl. Phys. Express* 11, 012703 (2018).
- [12] Wysocki, G., Bakhirkin, Y., So, S., Tittel, F. K., Hill, C. J., Yang, R. Q., Fraser, M. P., "Dual interband cascade laser based trace-gas sensor for environmental monitoring", *Appl. Opt.* 46(33), 8202-8210 (2007).
- [13] Ren, W., Luo, L., Tittel, F. K., "Sensitive detection of formaldehyde using an interband cascade laser near 3.6 μm ", *Sensors and Actuators B* 221, 1062-1068 (2015).
- [14] Ghorbani, R., Schmidt, F. M., "ICL-based TDLAS sensor for real-time breath gas analysis of carbon monoxide isotopes", *Opt. Express* 25(11), 12743-12752 (2017).
- [15] Lundqvist, S., Kluczynski, P., Weih, R., von Edlinger, M., Nähle, L., Fischer, M., Bauer, A., Höfling, S., Koeth, J., "Sensing of formaldehyde using a distributed feedback interband cascade laser emitting around 3493 nm", *Applied Optics* 51(25), 6009-6013 (2012).
- [16] Zheng, C., Ye, W., Sanchez, N. P., K. Gluszek, A., Hudzikowski, A. J., Li, C., Dong, L., Griffin, R. J., Tittel, F. K., "Infrared Dual-Gas $\text{CH}_4/\text{C}_2\text{H}_6$ Sensor Using Two Continuous-Wave Interband Cascade Lasers", *IEEE Phot. Technol. Lett.* 28(21), 2351-2354 (2016).
- [17] Dong, L., Li, C., Sanchez, N. P., Gluszek, A. K., Griffin, R. J., Tittel, F. K., "Compact CH_4 sensor system based on a continuous-wave, low power consumption, room temperature interband cascade laser", *Appl. Phys. Lett.* 108, 011106 (2016).
- [18] Villares, G., Wolf, J., Kazakov, D., Süess, M. J., Hugi, A., Beck, M., Faist, "On-chip dual-comb based on quantum cascade laser frequency combs", *J., Appl. Phys. Lett.* 107, 251104 (2015).
- [19] Jouy, P., Wolf, J. M., Bidaux, Y., Allmendinger, P., Mangold, M., Beck, M., Faist, "Dual comb operation of $\lambda \sim 8.2 \mu\text{m}$ quantum cascade laser frequency comb with 1 W optical power", *J., Appl. Phys. Lett.* 111, 141102 (2017).
- [20] Schliesser, A., Picqué N., Hänsch, T. W., "Mid-infrared frequency combs", *Nature Photon.* 6, 440-449 (2012).
- [21] Ideguchi, T., Holzner, S., Bernhardt, B., Guelachvili, G., Picqué, N., Hänsch, T. W., *Nature* 502, 355-358 (2013).
- [22] Dyksik, M., Motyka, M., Kurka, M., Ryczko, K., Misiewicz, J., Schade, A., Kamp, M., Höfling, S., Sęk, G., "Electrical tuning of the oscillator strength in type II InAs/GaInSb quantum wells for active region of passively mode-locked interband cascade lasers", *Jap. J. Appl. Phys.* 56, 110301 (2017).
- [23] Bagheri, M., Frez, C., Sterczewski, Ł. A., Gruidin, I., Fradet, M., Vurgaftman, I., Canedy, C. L., Bewley, W. W., Merritt, C. D., Kim, C. S., Kim, M., Meyer, J. R., "Passively mode-locked interband cascade optical frequency combs", *Scientific Reports* 8(1), 3322 (2018).
- [24] Vurgaftman, I., Meyer, J. R., Ram-Mohan, L. R., "Band parameters for III-V compound semiconductors and their alloys", *J. Appl. Phys.* 89(11), 5815-5875 (2001).
- [25] Ryczko, K., Sęk, G., Misiewicz, J., "Eight-band $k \cdot p$ modeling of InAs/InGaAsSb type-II W-design quantum well structures for interband cascade lasers emitting in a broad range of mid infrared", *J. Appl. Phys.* 114, 223519 (2013).
- [26] Ryczko, K., Sęk, G., "Polarization-independent gain in mid-infrared interband cascade lasers", *AIP Advances* 6, 115020 (2016).
- [27] Ryczko, K., Misiewicz, J., Höfling, S., Kamp, M., Sęk, G., "Optimizing the active region of interband cascade lasers for passive mode-locking", *AIP Advances* 7, 015015 (2017).